Biomech Model Mechanobiol (2009) 8:499–507
DOI 10.1007/s10237-009-0153-6

ORIGINAL PAPER

Darcian permeability constant as indicator for shear stresses in regular scaffold systems for tissue engineering

Petra Vossenberg · G. A. Higuera · G. van Straten · C. A. van Blitterswijk · A. J. B. van Boxtel

Received: 16 December 2008 / Accepted: 24 March 2009 / Published online: 10 April 2009
© Springer-Verlag 2009

Abstract The shear stresses in printed scaffold systems for tissue engineering depend on the flow properties and void volume in the scaffold. In this work, computational fluid dynamics (CFD) is used to simulate flow fields within porous scaffolds used for cell growth. From these models the shear stresses acting on the scaffold fibres are calculated. The results led to the conclusion that the Darcian (k_1) permeability constant is a good predictor for the shear stresses in scaffold systems for tissue engineering. This permeability constant is easy to calculate from the distance between and thickness of the fibres used in a 3D printed scaffold. As a consequence computational effort and specialists for CFD can be circumvented by using this permeability constant to predict the shear stresses. If the permeability constant is below a critical value, cell growth within the specific scaffold design may cause a significant increase in shear stress. Such a design should therefore be avoided when the shear stress experienced by the cells should remain in the same order of magnitude.

Keywords Shear stress · Printed scaffolds · Computational fluid dynamics · Permeability constants

P. Vossenberg · G. van Straten · A. J. B. van Boxtel
Systems and Control Group, Wageningen University,
P.O. Box 17, 6700 AA Wageningen, The Netherlands

P. Vossenberg · G. A. Higuera · C. A. van Blitterswijk
Department of Tissue Regeneration,
Institute for Biomedical Technology, University of Twente,
P.O. Box 217, 7500 AE Enschede, The Netherlands

P. Vossenberg (✉)
Food and Bioprocess Engineering Group,
P.O. Box 8129, 6700 EV Wageningen, The Netherlands
e-mail: petra.vossenberg@wur.nl

1 Introduction

Tissue engineering applies the principles of biology and engineering to the development of functional substitutes for damaged tissue such as skin, cartilage or bone (Langer and Vacanti 1993). The core materials used in tissue engineering are different types of cells, for example fibroblasts, chondrocytes or mesenchymal stem cells (MSCs).

To establish a tissue culture, expansion and differentiation of cells is needed. This expansion and differentiation should preferably occur in a physiological environment which is closer to the cells' native environment. To achieve this, bioreactor systems may be used. One way to culture cells in vitro is in a perfusion bioreactor housing a three-dimensional (3D) scaffold. Other options include two-dimensional (2D) polystyrene tissue culture flasks, spinner flasks, where the cells are usually grown on microcarriers, and hollow-fibre reactors, where the cells are attached to the outside of the fibres (Pörtner et al. 2005).

In a perfusion system, the cells may be attached to printed scaffolds (see Fig. 1 as an example), which can be fabricated using 3D printing technology consisting of fibres of the copolymers polyethylene oxide terephtalate (PEOT) and polybutylene terephtalate (PBT) with polyethylene glycol (PEG) starting blocks (Moroni et al. 2006). Many other types of scaffold are nowadays available with varying architectures, composite materials and surface chemistries. Scaffolds provide a large surface area that facilitates the attachment, survival, migration, proliferation and differentiation of cells (Muschler et al. 2004). Furthermore, the scaffold contains void spaces to allow mass transport to take place through convection and diffusion (Karande et al. 2004). The advantage of printed scaffolds is that they have a formally designed regular structure, which is reproducible. This offers the potential for greater control and a better prediction of the fluid flow within

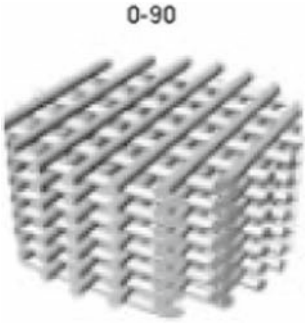

Fig. 1 Scaffold architecture with perpendicular fibres (Moroni et al. 2006)

the scaffold compared to random structures (Muschler et al. 2004). A possibility could therefore be to use the regular 3D printed scaffolds for the culture of undifferentiated MSCs, chondrocytes or endothelial cells and investigate the effect of fluid flow on the growth of the different cell types. If this concept is understood, a next step could be to cause specific cell differentiation of the MSCs as a result of a difference in fluid flow.

The flow of medium through the scaffold is necessary to provide the cells with nutrients and oxygen and flush out the metabolic products. The success of cell attachment to the scaffold depends on the flow regime. High flows cause high shear stress (Martin and Vermette 2005) and prevent attachment of cells to the scaffold surface, already attached cells may be damaged or hindered in proliferation. Shear stress is also considered as an important parameter for in vivo systems. Wang and Tarbell (2000) found by experiments for smooth muscle cells that with increasing shear stress the production of prostaglandins increased. The results of Wang and Tarbell (2000) indicate that the blood flow rate plays a role in the signal communication system from the blood vessels to the smooth muscle cells.

When designing a scaffold, the shear stress that acts on the fibres of the scaffold on which the cells grow must therefore be considered as a design parameter. Shear stress is proportional to the velocity gradient and is a function of design parameters such as fibre diameter and distance between the fibre centres and operational variables such as fluid velocity.

Martin et al. (2004) argue for the use computational techniques to predict the effect of flow conditions in bioreactors used for tissue engineering. Boschetti et al. (2006) apply computational fluid dynamics (CFD) calculations to a 3D-scaffold structure. Their work shows that the porosity, i.e. the void volume in the scaffold, is an important variable that affects the shear stress in scaffold systems. A conclusion from their work could be that prediction of the shear stress can only be obtained from CFD calculations. However, if we realize that the pressure drop caused by fluid-wall interaction in a structure is proportional to permeability of the structure, then it is also an option to link the shear stress to permeability constants. Wang and Tarbell (2000) use the permeability constant from Darcy's law to derive the average shear stress from experiments on a collagen gel. The permeability constant was determined using the viscosity of the perfusing medium, the measured volumetric flow rate, the cross-sectional area and the imposed pressure drop over the length of the reactor.

In this work the shear stress in a regular printed scaffold is calculated with CFD. CFD calculations demonstrated, just as in the work of Boschetti et al. (2006), that the shear stress varies with the porosity of the scaffold. The Darcian permeability constant in the Forchheimer equation showed good results as predictor of shear stress and was independent of scaffold parameters like porosity. With these findings the shear stress in scaffolds can directly be predicted from the Darcian permeability constant without doing extensive CFD calculations.

Actual measurement of shear stress in the dimensions of scaffolds used for cell growth is not yet possible. The only experimental option is to investigate the cells' phenotype in response to shear stress. The focus of this work, however, is on finding a relationship between scaffold design and shear stress. To obtain a visual indication on how and where cells grow on a regular 3D printed scaffold, goat mesenchymal stem cells (gMSCs) were cultivated in a dynamic perfusion system.

2 Methods

2.1 CFD-calculations

In the fluid domain, the Navier–Stokes equation for incompressible fluid dynamics was solved. The equation is as follows:

$$\begin{aligned} &\rho\frac{\partial u}{\partial t} - \eta\nabla^2 u + \rho(u\cdot\nabla)u + \nabla p = F \\ &\nabla\cdot u = 0 \end{aligned} \tag{1}$$

where ρ is the fluid density (kg m^{-3}), u is the velocity field (m s^{-1}), t is the time (s), η is the dynamic viscosity of the fluid (kg m^{-1} s^{-1}), ∇ is the del operator, p is the pressure (Pa) and F represents other forces (gravity or centrifugal force) (in this case $F = 0$).

The steady state equation was applied because the cell cultivation in a perfusion system is mainly in steady state. Furthermore, when the system is disturbed, it will restore itself quickly.

Assuming the fibres of the scaffold and the wall of the bioreactor to be rigid and impermeable, no-slip boundary conditions were applied to the surfaces of the fibres and the wall of the bioreactor. The culture medium flows in the positive z-direction. At $z = 0$, the boundary condition was set to a

specific inlet velocity with only a z-component. The boundary condition at the outlet was set to normal flow/pressure with null pressure.

For laminar flow, the wall shear stress is defined by the normal velocity gradient at the wall as:

$$\tau_w = \eta \frac{\partial v}{\partial n} \tag{2}$$

where τ_w is the wall shear stress (Pa), η is the dynamic viscosity of the fluid (kg m^{-1} s^{-1}), v is the fluid velocity (m s^{-1}) and n is the x-, y- and z-direction (m).

CFD models of the fluid flow through different scaffold designs were set-up and solved in the modelling package COMSOL Multiphysics 3.3. The computations were carried out on a PC with 10 Gb of RAM. The solver GMRES, which is an iterative solver, was used to simulate the fluid flow through the different scaffold designs. A predefined mesh size, called 'fine', was used to divide the fluid domain into elements. The maximum element size scaling factor for this predefined mesh was 0.8, the element growth rate 1.45, the mesh curvature factor 0.5, the mesh curvature cut-off 0.02 and the resolution of narrow regions 0.6.

In 3D the total wall shear stress is calculated based on the shear stress acting in the x-, y- and z-direction using Pythagoras' theorem. CFD calculations with COMSOL allow the export of shear stress values in the x-, y- and z-direction at points along the edges which make up the scaffold model. Data from COMSOL was exported to calculate the average and maximum shear stress found for specific scaffold designs. The average shear stress is an indication of the amount of shear stress that most cells will likely experience within the scaffold system. The maximum shear stress is an indication of the extremities of the scaffold system with respect to the shear stress. Some cells may experience these extremities within the scaffold system.

2.2 Porosity and permeability constants

One-way to characterise a scaffold design is in terms of porosity (ε) (Boschetti et al. 2006), whereby the porosity is defined as the percentage of void volume within the total volume of the scaffold. For a scaffold section, for which the width of the section equals the length and two fibres are present per layer, the porosity is given by:

$$\varepsilon = \left(1 - \frac{2\pi r^2 n_l}{wh}\right)100 \tag{3}$$

where r is the fibre radius (m), w is the width of scaffold section (m), n_l is the number of fibre layers and h is the height of scaffold section (m).

Permeability is a measure of the ability of a porous medium to transmit fluids through its interconnected pores or channels. Two permeability parameters, known as the Darcian, k_1, and the non-Darcian, k_2, permeability constants, can be found in the Forchheimer equation (Innocentini et al. 1999). The Darcian permeability constant is related to the pure laminar flow properties while the non-Darcian permeability constant represents deviations from laminar flow. The Forchheimer equation states that for an uncompressible fluid, the pressure drop through a rigid and homogeneous porous medium is given by:

$$\frac{\Delta P}{L} = \frac{\eta}{k_1} v + \frac{\rho}{k_2} v^2 \tag{4}$$

where ΔP is the pressure drop (Pa), L is the path length (m), η is the dynamic viscosity of the fluid (kg m^{-1} s^{-1}), k_1 is the Darcian permeability constant (m^2), v is the fluid velocity (m s^{-1}) and k_2 is the non-Darcian permeability constant (m).

Ergun proposed empirical expressions to describe the two permeability parameters for packed columns made of grains (Innocentini et al. 1999; Nield and Bejan 2006). These expressions are:

$$k_1 = \frac{\varepsilon^3 d^2}{150(1-\varepsilon)^2} \tag{5}$$

$$k_2 = \frac{\varepsilon^3 d}{1.75(1-\varepsilon)} \tag{6}$$

where ε is the porosity (as defined by Eq. 3) and d is the mean particle diameter of the medium in the packed column (m).

In scaffolds the flow is around fibres instead of around grains that make up a packed bed. This means that to evaluate k_1 and k_2 the mean particle diameter of the grains (d) has to be replaced by a structural property of the scaffold. Here d is defined as the diameter of the scaffold fibres as representation of the effective scale of the microstructure.

If the fluid velocity through the scaffold is taken to be 100 µm s^{-1} and the fibre radius 75 µm, a Reynolds number equal to 7.5×10^{-3} results. Turbulent flow occurs for a Reynolds number larger than 1. This leads to the conclusion that while k_1 will be relevant in the transmittance of fluid through a scaffold and with a velocity of these dimensions, k_2 will not be.

2.3 Cell cultivation

Janssen et al. (2006) developed a perfusion bioreactor system capable of producing clinically relevant volumes of tissue-engineered bone on macro porous biphasic calcium phosphate scaffolds. This system was used for the cultivation of gMSCs on regular 3D printed scaffolds, consisting of fibres of the copolymers PEOT and PBT with PEG starting blocks and fabricated as described by Moroni et al. (2006). The k_1 value in the system was 2.28×10^{-10} m^2. 10 million gMSCs were used to dynamically seed a scaffold for 4 hours with a superficial velocity of 100 µm s^{-1}. During cultivation medium was pumped through the scaffold with

the same superficial velocity as was used during seeding. The medium (300 ml) was refreshed every 3 days.

After 14 days of cultivation the scaffold was removed from the system and fixed in 1.5% glutaraldehyde, 0.14 M cacodylic buffer, pH 7.2–7.4 adjusted with 1 M hydrochloric acid (HCl). The fixed scaffold was placed in phosphate buffered saline (PBS) to cut into smaller sections. The sections were dehydrated and subsequently dried with a CO_2 critical point dryer, CPD 030 (Balzers). The sections were coated with gold using a sputter coater, 108 Auto (Cressington) before examining them using a scanning electron microscope (SEM), XL 30 SEM FEG (Philips) at 10 kV.

3 Results and discussion

3.1 CFD-calculations

In Fig. 2a the shear stress acting on the side edge of a fibre present in two layers at different heights in a scaffold is given. The scaffold consists of five crossing fibres. Figure 2b is a schematic drawing of the fibre and cross-fibres for which the shear stress values are displayed in Fig. 2a. The maxima of the curves in Fig. 2a are the shear stress values found within the pores of the scaffold. The minima are the shear stress values found where two fibres cross perpendicularly. The values left in the graph concern the shear stress at positions along the fibre close to the wall and the other values the shear stress at positions towards the centre of the scaffold. The results indicate that the "wall" effect concerns only a small part of the fibre. Along the rest of the fibre, a repetitious shear stress pattern can be observed. This conclusion is also valid for scaffolds with other fibre diameters and distances between the fibres.

Scaffolds used for tissue engineering concern over twenty crossing fibres in each layer. For such systems the "wall" effect is negligible. Therefore the shear stress is well represented by a section of the scaffold as given in Fig. 3. In Fig. 3 a small section of the scaffold is shown. The width and length of the section are equal to twice the distance between the centres of the fibres. The boundary conditions applied to the four sides are slip/symmetry.

Using this approach it is possible to simulate the fluid dynamics within scaffolds that consist of thinner fibres, more

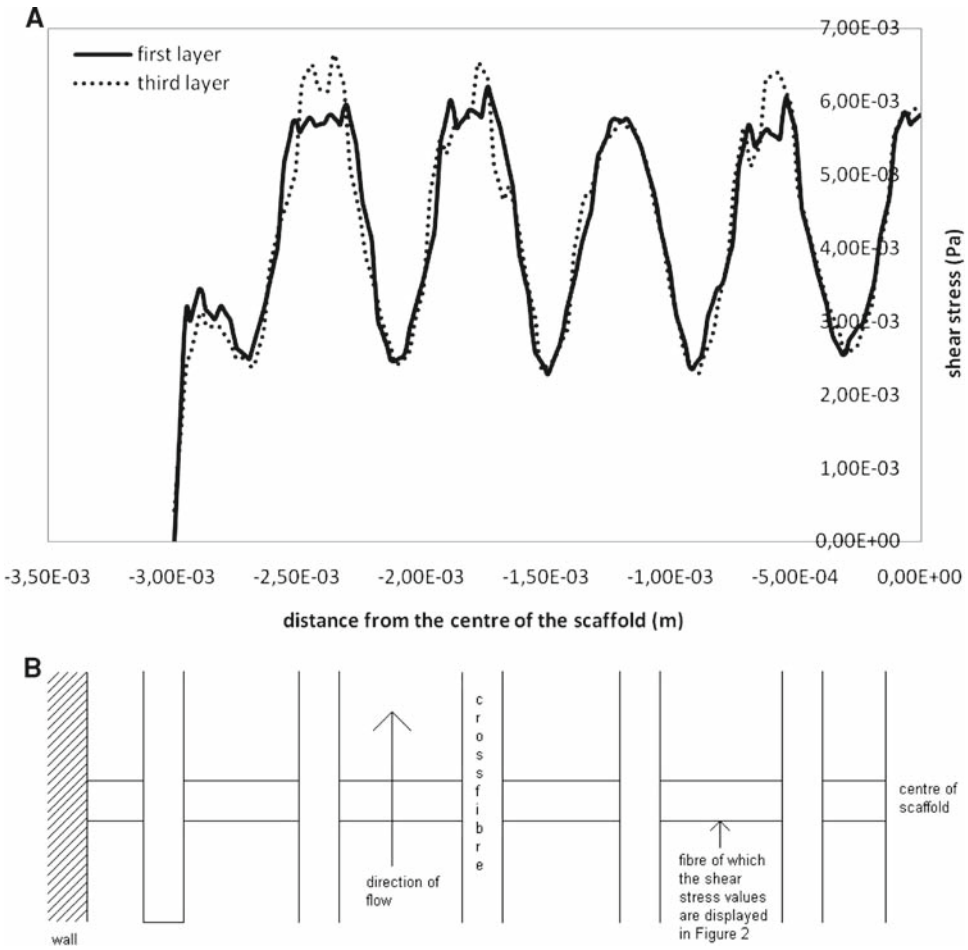

Fig. 2 Shear stress acting on the side edge of fibres present in two layers at different heights in a scaffold. **a** Shear stress values at the fibres. **b** Position of cross-fibres and wall in the system. The scaffold consists of five crossing fibres. Inlet velocity = 100 μm s^{-1}. Radius of fibres = 130 μm. Distance between the centres of the fibres = 600 μm

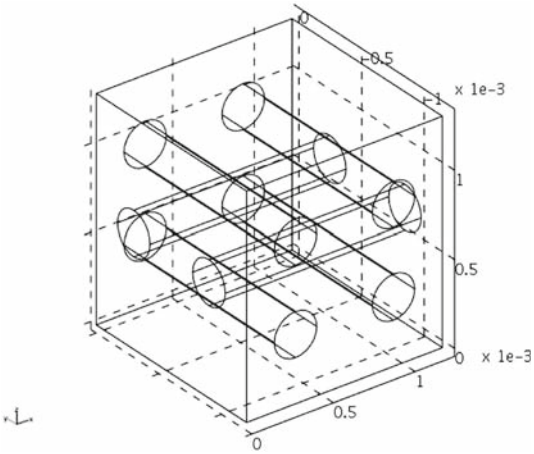

Fig. 3 A small section of a scaffold containing three layers of fibres at 90°, length and width of section = 1.2 mm, height of section = 1.3 mm, radius of fibres = 130 µm, distance between centre of fibres = 600 µm

layers of fibres and smaller distances between the fibre centres than the scaffold used for the calculations of which the outcomes are displayed in Fig. 2a. The velocity profile within a scaffold section consisting of 32 layers of fibres, with a fibre radius of 75 µm and a distance between the fibre centres of 300 µm can be seen in Fig. 4a. Figures 4b and c are close-ups for the velocity profile in between two crossing fibres and at a crossing fibre.

3.2 Porosity and permeability constants

As seen in Fig. 5 the average and maximum total shear stress increases with decreasing porosity. These results are in line with the findings of Boschetti et al. (2006) and were expected as with decreasing porosity there is less space for the fluid to flow causing steeper velocity gradients. Hence higher shear stresses will act on the surfaces of the scaffold fibres.

In the studied range, the maximum total shear stress is between 2.5 and 4.1 times larger than the average total shear stress. The difference between the maximum and average total shear stress increases with decreasing porosity. Below 50% porosity and certainly below 40% porosity, the total shear stress starts to rise significantly.

The relationship between the average and maximum total shear stress and porosity depends on the distance between the centres of the fibres. This means that porosity alone is not a sufficient indicator for characterising the shear stress within the scaffold. Another scaffold characteristic is therefore necessary. Ideally, this scaffold characteristic should allow the estimation of the average and maximum shear stresses found within the scaffold design without having to carry out CFD calculations.

When the average and maximum shear stresses are plotted against the Darcian (k_1) permeability constant, the dependence of the average and maximum shear stress on the distance between the centres of the fibres becomes minimal (Fig. 6). k_1 can thus be used as a scaffold characteristic to estimate the average and maximum shear stress acting on the fibres of a scaffold without having to carry out CFD calculations. The permeability constant allows the quick assessment of the effect of scaffold design on the shear stresses acting on the fibres of the scaffold. The figure shows that the maximum and average shear stresses are nearly constant for high values of k_1. For low values the scaffold design is very shear

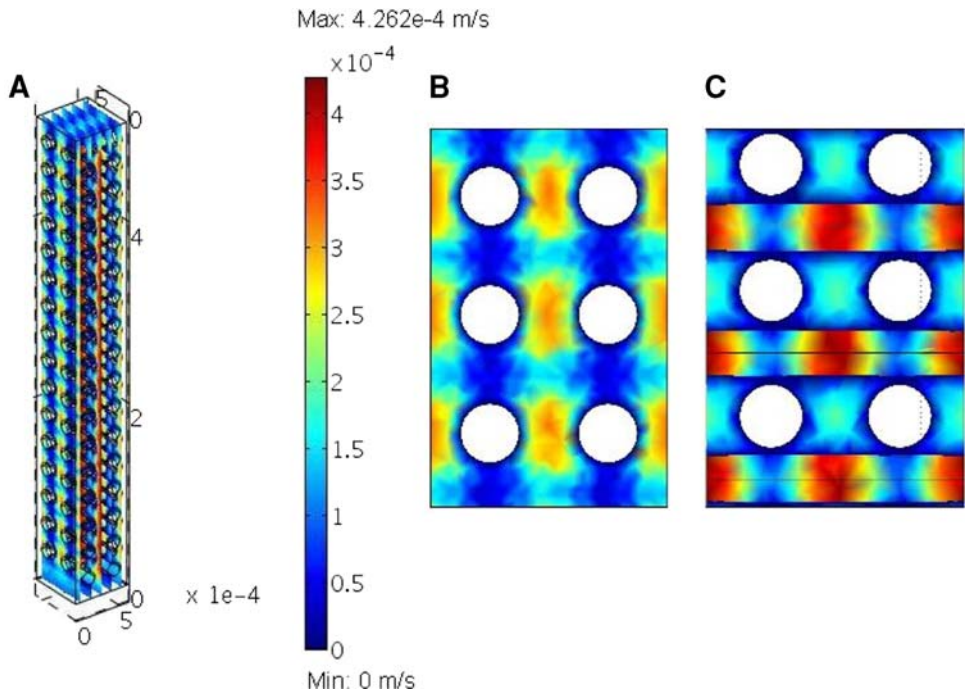

Fig. 4 Velocity profile of the fluid within a porous scaffold consisting of 32 layers of fibres, radius of fibres = 75 µm, distance between fibre centres = 300 µm. Inlet velocity = 100 µm s^{-1}. **a** Velocity profile within complete scaffold. **b** Close-up of the flow profile in between two crossing fibres. **c** Close-up of the profile at a crossing fibre

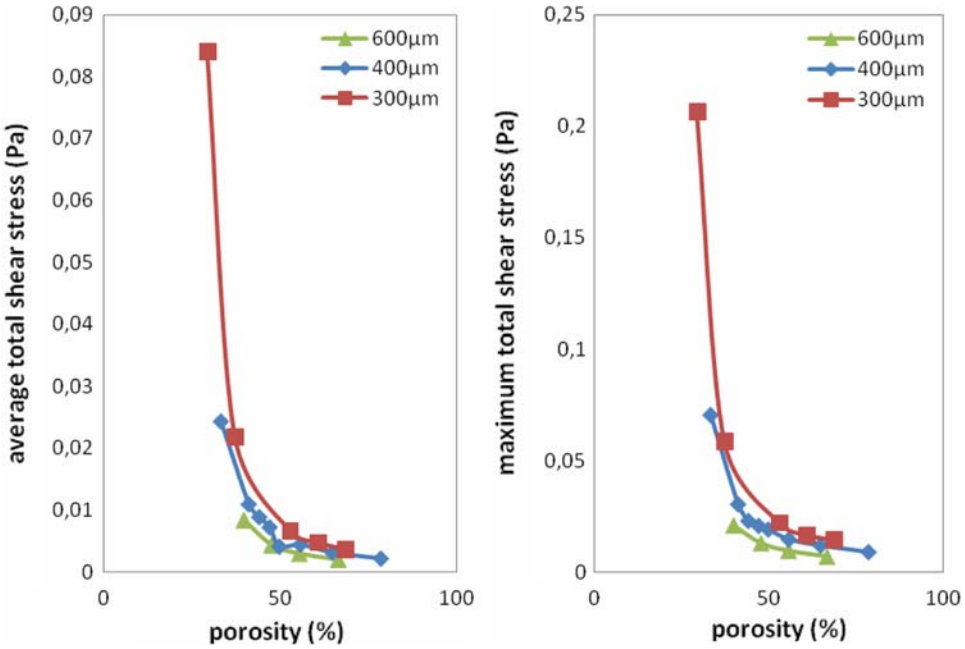

Fig. 5 Average and maximum total shear stress as a function of relative porosity at varying distances between the centres of the fibres. Inlet velocity = 100 µm s^{-1}

sensitive, which can be useful when designing scaffolds for experiments where shear stress wants to be actively induced.

Below a Darcian (k_1) permeability constant of about 1×10^{-10} m^2, small changes in porosity or changes in the shortest distance between the fibres have a large effect on the average total shear stress. These values for the k_1 can thus be seen as critical values for an inlet velocity of 100 µm s^{-1}.

Wang and Tarbell (1995) use the Brinkman model to calculate the average wall shear stress on smooth muscle cells located in an artery wall. The muscle cells are modelled as a periodic array of cylindrical objects. They express the average shear stress as a function of the cell concentration (C), the Darcian permeability constant (k_1), the fluid velocity (v) and the dynamic viscosity of the fluid (η):

$$\tau_w = \frac{B\eta v}{\sqrt{k_1}} \tag{7}$$

where the constant B is a function of the cell volume (C) in a volume element:

$$B = \frac{4}{\pi} \frac{1 - 0.319285C^2 - 0.043690C^4}{\sqrt{(1 - C - 0.305828C^4)(1 + C - 0.305828C^4)}} \tag{8}$$

At a cell concentration of zero, B becomes equal to $4/\pi$. A plot of the Brinkman model at zero cell concentration can be seen in Fig. 6. We can see that at high values of k_1 the Brinkman model predicts the computed average shear stress data. At low values of k_1 the Brinkman model at zero cell concentration starts to deviate.

In our work instead of the cell concentration, the porosity of the scaffold (ε) is used. ε is a function of the fibre diameter and the distance between the centres of the fibres. With $\varepsilon = 1 - C$, the Darcian permeability constant defined in Eq. 5 becomes:

$$k_1 = \frac{(1 - C)^3 d^2}{150C^2} \tag{9}$$

The expression shows that two different scaffold structures with the same value for C or ε can have different values for k_1. Therefore plotting the average shear stress against the Darcian permeability constant will yield different lines for the shear stress depending on the fibre diameter and the distance between the centres of the fibres. However, in Fig. 6 we see only small variations between the lines. The reason for this result might be the complexity of the scaffold structure with crossing fibres compared to the system considered by Wang and Tarbell (1995) with parallel fibres. In addition, Swartz and Fleury (2007) suggest that differences arise between the solution from the Navier–Stokes equation, as used in our work, and the Brinkman model, as used by Wang and Tarbell (1995), because the Navier–Stokes equation takes into account the exact location and dimensions of the fibres.

The average ($\tau_{w\mathrm{avg}}$) and maximum ($\tau_{w\mathrm{max}}$) shear stress data in Fig. 6 were fitted with the following power functions:

$$\tau_{w\mathrm{avg}} = 9.82 \times 10^{-12} k_1^{-0.914} \tag{10}$$

$$\tau_{w\mathrm{max}} = 3.36 \times 10^{-10} k_1^{-0.807} \tag{11}$$

Equations 10 and 11 could be used by scaffold designers to quickly have an indication of what average and maximum shear stress values one can expect in a specific scaffold design.

The local shear stress is also linked to the permeability constant k_1. Figure 7 shows the local shear stress acting on the side edge of a fibre, which is crossed by two other

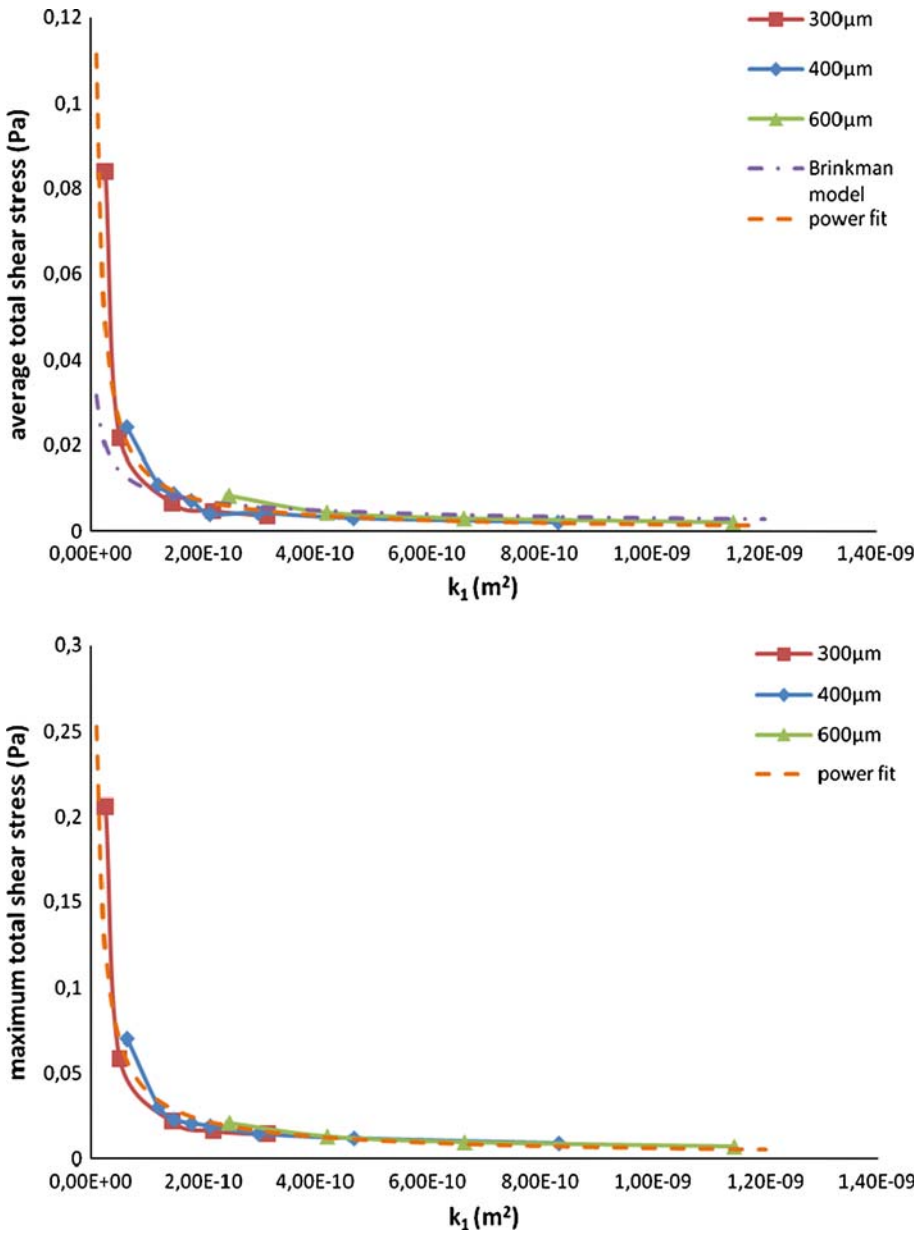

Fig. 6 Average and maximum total shear stress as a function of the Darcian permeability constant, k_1, at varying distances between the centres of the fibres. Inlet velocity = 100 µm s^{-1}. The average total shear stress graph includes a fit based on the Brinkman model at zero cell concentration. Both the average and maximum total shear stress graphs include a power function fit of the computed data

fibres at 2×10^{-4} and 6×10^{-4} m, for varying k_1 values. As was seen in Fig. 6 the shear stress decreases for increasing k_1 values. The large difference in shear stresses for a k_1 value of 1.20×10^{-10} and 6.35×10^{-11} m^2 could also be observed in Fig. 6. As was mentioned above, k_1 values below 1×10^{-10} m^2 are critical values as small changes in the scaffold dimensions (i.e. a small increase in the diameter of the fibre due to cell growth) will have a large effect on the shear stress.

The shear stress is related to the linear flow velocity within the scaffold. The graph of average total shear stress as a function of the Darcian (k_1) permeability constant therefore depends on the inlet velocity. In Fig. 8 the effect of varying linear inlet velocity on the average and maximum total shear stress is shown. The graphs display the average and maximum total shear stress set out against k_1 for two different linear inlet velocities.

As the inlet velocity is changed from 100 µm s^{-1} to 300 µm s^{-1} the average and maximum total shear stresses are also tripled. This result, which corresponds with the work of Wang and Tarbell (1995), indicates that the flow is in the laminar region (as was expected based on the low Reynolds number), where the wall shear stress is directly proportional to the normal velocity gradient at the wall. This leads to the conclusion that as long as the flow is laminar the average and maximum total shear stress can be calculated for different inlet velocities from the shear stress found for an inlet velocity of 100 µm s^{-1}.

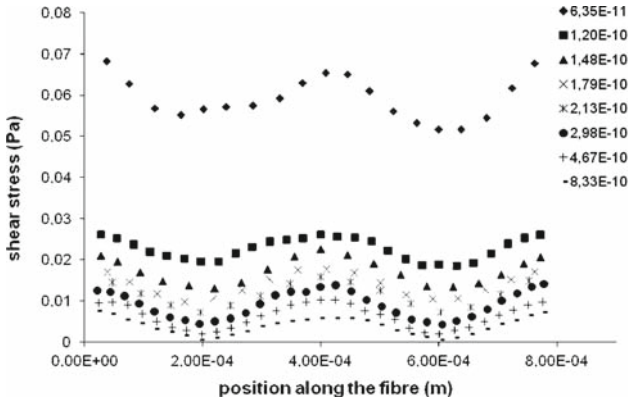

Fig. 7 Shear stress acting on the side edge of a fibre, which is crossed by two other fibres at 2×10^{-4} and 6×10^{-4} m , for varying k_1 values. Distance between the centres of the fibres = 400 µm. Inlet velocity = 100 µm s^{-1}

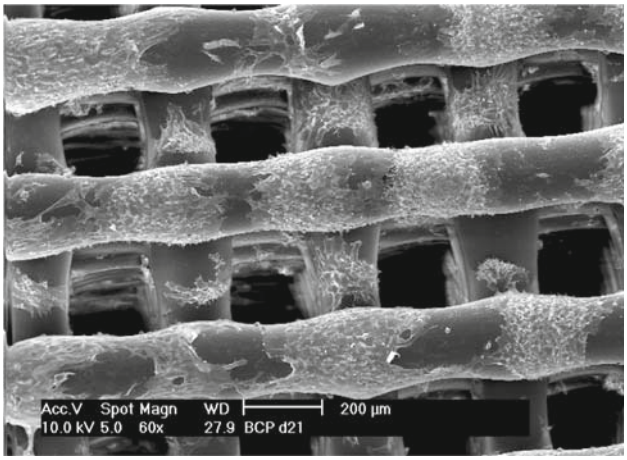

Fig. 9 Scanning electron microscope (SEM) photograph of goat mesenchymal stem cells (gMSCs) and extracellular matrix (ECM) attached to printed scaffolds, consisting of fibres of the copolymers polyethylene oxide terephtalate (PEOT) and polybutylene terephtalate (PBT) with polyethylene glycol (PEG) starting blocks. The k_1 value in this system was 2.28×10^{-10} m^2, photograph was taken after 14 days of cultivation with a superficial medium flow velocity of 100 µm s^{-1}

3.3 Cell cultivation

Figure 9 shows a SEM photograph of gMSCs and extracellular matrix (ECM) attached to a printed scaffold. It can be seen that cell growth and ECM deposition results in a slight increased fibre diameter and decreased porosity. The Darcian permeability constant will therefore decrease. When a scaffold design is made whereby the permeability constant is around or below the critical value, cell growth within the scaffold may cause a significant increase in shear stress. Such a design should therefore be avoided when the shear stress experienced by the cells should remain in the same order of magnitude.

Cell growth may occasionally take place from one fibre to the next. The shear stress experienced by these cells were not incorporated in the CFD calculations as the largest amount of cells cover the fibres and lead to an increase in fibre diameter. In addition, non-smooth cell coverage of the scaffold may increase the friction factor between the fluid and the scaffold. The effect of non-smooth deposition is difficult to predict as there are so many possible options for coverage.

Figure 9 also gives a visual indication that cells grow the best around the crossings of the fibres. The location of

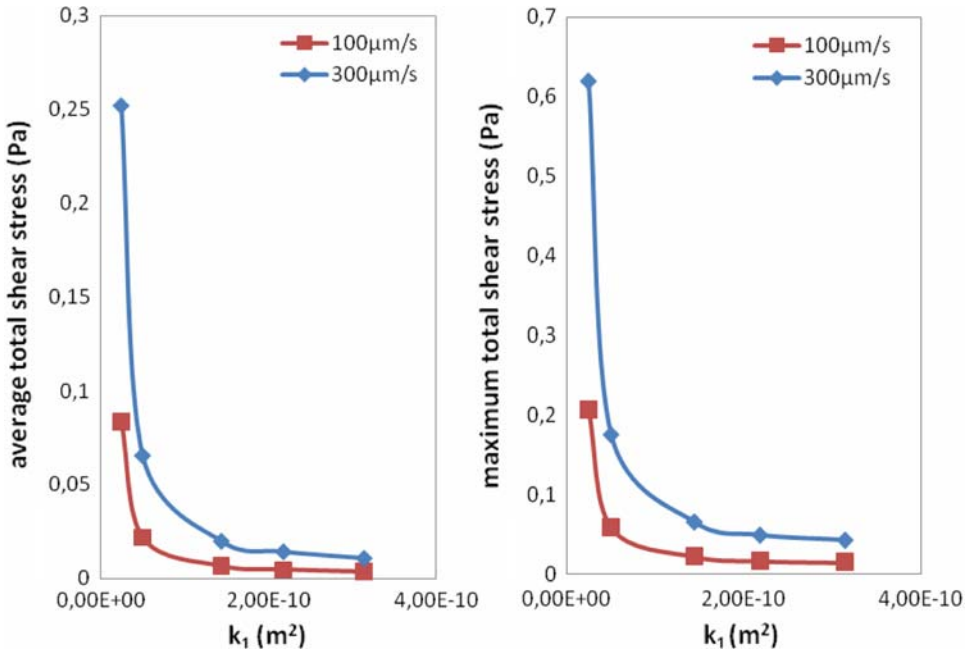

Fig. 8 Effect of a difference in linear inlet velocity on the average and maximum total shear stress. The average total shear stress is displayed as a function the Darcian permeability constant, k_1, at a distance of 300 µm between the centres of the fibres. Inlet velocities = 100 and 300 µm s^{-1}

low shear stress values at these points is one possible reason for the higher cell concentration at these fibre crossings. Another possibility is that the geometry around the fibre crossings is preferential for cell growth. To distinct both mechanisms additional experiments are required. For example, an experiment in which very low values of shear stress are used. Low values of shear stress can be achieved either by varying the design parameters of the scaffold such as by increasing the distance between the fibres or by varying the operational variables such as by decreasing the fluid velocity. If the geometric properties of the crossings are dominant for cell growth, then the cells will again have preference for the crossing. If shear stress is dominant, then a uniform coverage of the fibres will occur.

4 Conclusions

Shear stress is an important variable for in vivo systems and in vitro cultivation of cells in bioreactors. Too high shear stress prevents attachment of the cells to the scaffold structures, may damage cells and hinder proliferation. Modern computational techniques as CFD allow the calculation of the shear stress in different scaffolds. However, the CFD calculation request for a high computational capacity and specialists to translate the scaffold structure into a CFD computer program.

By performing CFD calculations on printed scaffolds, this work demonstrates that CFD calculations can be circumvented in the future by using the Darcian (k_1) permeability constant as indicator for shear stresses. Calculation of this constant from Eqs. 3, 5, 10 and 11 allows a quick assessment of the effect of scaffold design on the average and maximum shear stress acting on the fibres of a printed scaffold. If the permeability constant is below a critical value, the shear stress will be too high for effective cultivation. Moreover, with cell growth at the fibres of the scaffold the permeability of the scaffold can decrease and may result in a significant increase in shear stress if the permeability constant is around the critical value. Such a design should therefore be avoided when the shear stress experienced by the cells should remain in the same order of magnitude.

We expect that the Darcian permeability constant can play a similar role in estimating the shear stress in other scaffold structures and also for characterizing irregular systems. However, these applications must be validated.

References

Boschetti F, Raimondi MT, Migliavacca F, Dubini G (2006) Prediction of the micro-fluid dynamic environment imposed to three-dimensional engineered cell systems in bioreactors. J Biomech 39:418–425. doi:10.1016/S0021-9290(06)85506-5

Innocentini MDM, Salvini VR, Macedo A, Pandolfelli VC (1999) Prediction of ceramic foams permeability using Ergun's equation. Mater Res 2:283–289. doi:10.1590/S1516-14391999000400008

Janssen FW, Oostra J, van Oorschot A, van Blitterswijk CA (2006) A perfusion bioreactor system capable of producing clinically relevant volumes of tissue-engineered bone: in vivo bone formation showing proof of concept. Biomaterials 27:315–323. doi:10.1016/j.biomaterials.2005.07.044

Karande TS, Ong JL, Mauli-Agrawal C (2004) Diffusion in musculoskeletal tissue engineering scaffolds: design issues related to porosity, permeability, architecture, and nutrient mixing. Ann Biomed Eng 32(12):1728–1743. doi:10.1007/s10439-004-7825-2

Langer R, Vacanti JP (1993) Tissue engineering. Science 260(5110): 920–926. doi:10.1126/science.8493529

Martin Y, Vermette P (2005) Bioreactors for tissue mass culture: design, characterization, and recent advances. Biomaterials 26:7481–7503. doi:10.1016/j.biomaterials.2005.05.057

Martin I, Wendt D, Heberer M (2004) The role of bioreactors in tissue engineering. Trends Biotechnol 22(2):80–86

Moroni L, Poort G, van Keulen F, de Wijn JR, van Blitterswijk CA (2006) Dynamic mechanical properties of 3D fiber-deposited PEOT/PBT scaffolds: an experimental and numerical analysis. J Biomed Mater Res A 78A(3):605–614. doi:10.1002/jbm.a.30716

Muschler GF, Nakamoto C, Griffith LG (2004) Engineering principles of clinical cell-based tissue engineering. J Bone Joint Surg 86(7):1541–1558

Nield DA, Bejan A (2006) Convection in porous media. Springer, New York

Pörtner R, Nagel-Heyer S, Goepfert C, Adamietz P, Meenen NM (2005) Bioreactor design for tissue engineering. J Biosci Bioeng 100(3):235–245. doi:10.1263/jbb.100.235

Swartz MA, Fleury ME (2007) Interstitial flow and its effects in soft tissues. Annu Rev Biomed Eng 9:229–256. doi:10.1146/annurev.bioeng.9.060906.151850

Wang DM, Tarbell JM (1995) Modeling interstitial flow in an artery wall allows estimation of wall shear stress on smooth muscle cells. J Biomech Eng 117:358–363. doi:10.1115/1.2794192

Wang S, Tarbell JM (2000) Effect of fluid flow on smooth muscle cells in a 3-dimensional collagen gel model. Arterioscler Thromb Vasc Biol 20:2220–2225